

pound-elastic scattering. Compound-elastic scattering has therefore been calculated, using the Hauser-Feshbach method, with the penetration factors obtained from the optical absorption cross section itself in the usual way. Partial waves up to $l=6$ are included, and allowance is made for nonzero target spin ($\text{Cu}^{63,65}$: spin $3/2$). It is assumed that only the entrance channel is open, which will be a good approximation at 1 MeV and a fair approximation even up to 2–3 MeV, as will be seen from the reaction cross sections quoted in Fig. 2.

The effect of compound-elastic scattering on the angular distributions at 1 MeV is shown by the dashed lines in Figs. 9 and 10. The cross section is increased by a factor of the order 1.5–2.0. Considering that the optical parameters have not been directly chosen to fit these angular distributions in detail, the corrected curves fit the data surprisingly well. The errors in the data (not shown) may be of the order of 10% or more (including multiple-scattering corrections).

As an estimate of the average¹⁷ effect of compound-

¹⁷ Compare with possible coherent statistical effects in the compound nucleus, as mentioned in the introduction.

nuclear processes on the polarization, the unpolarized cross section (which appears in the denominator) has been corrected to allow for the compound-elastic scattering. As an approximation, we take the ratio of corrected to uncorrected angular distributions at 55° and 90° at 1 MeV from Figs. 9 and 10, and apply this ratio uniformly throughout the energy range 200–1600 keV. The polarization, corrected in this way for compound-elastic scattering, is plotted as the dashed lines in Figs. 3–8. It is clear that the correction is quite significant.

ACKNOWLEDGMENTS

The author very gratefully acknowledges the generous collaboration of the late Frank Bjorklund, and of others of his colleagues at the Lawrence Radiation Laboratory who have assisted in performing these calculations or in discussing the results. Thanks are also due to E. A. Christiansen for assistance with the compound-elastic calculations, and to R. W. Humphrey for much useful discussion.

High-Energy Gamma Rays and Low-Energy Protons and Deuterons from $\text{C}^{12} + p$ for $E_p = 14\text{--}20$ MeV*

E. K. WARBURTON† AND H. O. FUNSTEN

Palmer Physical Laboratory, Princeton University, Princeton, New Jersey

(Received July 2, 1962)

The 90° yield of gamma rays from proton bombardment of C^{12} was studied for proton energies between 14 and 20 MeV. Gamma rays are observed corresponding to the ground-state decay of the C^{12} 4.43-, 12.7-, and 15.1-MeV levels and from the $\text{C}^{12}(p,\gamma_0)\text{N}^{13}$ reaction. Three resonances are observed in the yield of the 15.1-MeV gamma ray. These resonances correspond to N^{13} levels at 18.1, 18.65, and 19.8 MeV. The N^{13} 18.1-MeV level has a width of 330 ± 100 keV in the center-of-mass system. The other two levels have widths less than 200 keV. The yields of the 4.43- and 12.7-MeV gamma rays reveal little or no structure. The excitation function of the $\text{C}^{12}(p,\gamma_0)\text{N}^{13}$ reaction also shows little structure. Angular distributions and absolute integrated cross sections for the $\text{C}^{12}(p,p')\text{C}^{12}$ reaction are given for the C^{12} 12.7-MeV level with $E_p = 17.5, 19.5$, and 20 MeV and for the C^{12} 15.1-MeV level with $E_p = 19.5$ MeV. The latter is approximately symmetrical about 90° which suggests possible contribution from the compound nucleus reaction mechanism. Comparison of the cross sections for $\text{C}^{12}(p,p'\gamma)\text{C}^{12}$ and $\text{C}^{12}(p,p')\text{C}^{12}$ gives $\Gamma_\gamma/\Gamma = 0.027 \pm 0.007$ for the C^{12} 12.7-MeV state and 1.15 ± 0.3 for the C^{12} 15.1-MeV state. The yield of the $\text{C}^{12}(p,d)\text{C}^{11}$ reaction was measured by the stacked foil technique from threshold ($E_p = 17.85$ MeV) to 19.8 MeV. There is no evidence for structure. Angular distributions are given for the $\text{C}^{12}(p,d)\text{C}^{11}$ reaction for $E_p = 19.3, 19.5$, and 20.0 MeV. The results are compared to previous work on the $\text{B}^{11}(d,n)\text{C}^{12}$ reaction and it is concluded that the contribution of the compound nucleus reaction mechanism to either reaction is most likely small for the bombarding energies in question.

I. INTRODUCTION

ALTHOUGH extensive experimental data on the inelastic scattering of 15–20 MeV protons from light nuclei have become available in recent years,¹

* This work was supported by the U. S. Atomic Energy Commission, the Higgins Scientific Trust Fund, and the Air Force Office of Scientific Research.

† Present Address: Brookhaven National Laboratory, Upton, New York.

¹ G. Schrank, E. K. Warburton, and W. W. Daehnick, *Phys. Rev.* **127**, 2159 (1962); and references therein.

there are very few data on the scattering from levels above 10-MeV excitation energy. Scattering from levels with excitation energies which are a large fraction of the bombarding energy should show some distinctive features because of the low energy of the outgoing protons. For instance, it is expected that the direct-interaction cross section would be relatively low for such reactions since the high values of outgoing orbital angular momentum (and thus incoming orbital angular momentum) which contribute the major part of the

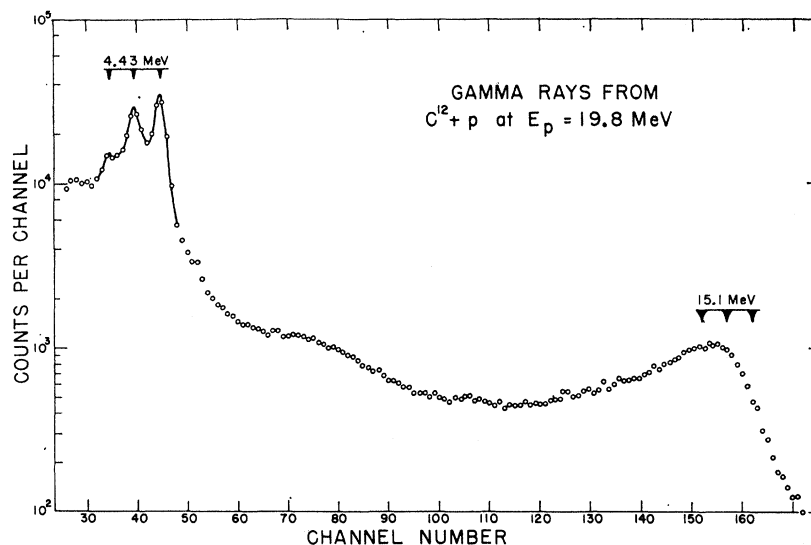


FIG. 1. Pulse-height spectrum of the gamma rays from $C^{12} + p$ at $E_p = 19.8$ MeV. The spectrum was taken with a 5-in. diam by 4-in. long NaI(Tl) crystal at 90° to the beam.

direct-interaction cross section for scattering from low-lying states will be suppressed by the centrifugal barrier in this case. The action of the centrifugal barrier on the high partial waves is also expected to cause the angular distributions to be flattened out since rapid variations of the differential cross section with angle demand a large contribution from high partial waves. On the other hand, compound nucleus formation should not be suppressed as much as the direct interaction cross section. This is so because the density of compound nucleus states is high enough in the region of excitation we are considering so that there should be compound nuclear states of low J available which can be formed by low values of proton orbital angular momenta for which the centrifugal barrier is not too high.

The $C^{12}(p,p')C^{12}$ (12.7-MeV level) and $C^{12}(p,p')C^{12}$ (15.1-MeV level) reactions initiated with incident proton energies in the range 14–20 MeV were chosen as a convenient testing ground for these considerations. Both levels are excited strongly by the (p,p') reaction and both emit ground-state gamma rays which can be used to obtain excitation functions for the reactions.

Detailed studies of the scattering^{2,3} of protons from the C^{12} ground state and first excited state and optical-model analysis of these results^{3,4} suggest the possible influence of resonances in the compound nucleus on the differential cross sections. However, if present, these resonances contribute a relatively small amount to the total cross sections and so are difficult to study by these reactions. In contrast, it was expected that the effect of these resonances (if present) might appear more strongly in the $C^{12}(p,p')C^{12}$ (12.7- and 15.1-MeV level)

reactions for the reasons given above. Thus, the possibility of studying the interplay of the direct interaction and compound nucleus reaction mechanisms provided the main motive for the investigation of inelastic proton scattering from the C^{12} 12.7- and 15.1-MeV levels which is reported here.

The $C^{12}(p,\gamma_0)N^{13}$ and $C^{12}(p,d)C^{11}$ reactions were also investigated. The primary purpose of this work was to see whether the excitation curves for these reactions had any features in common with the (p,p') results. However, these reactions are interesting in their own right. For instance, it is of interest to compare the $C^{12}(p,\gamma_0)N^{13}$ results with current ideas on photonuclear reactions, while a comparison of the $C^{12}(p,d)C^{11}$ reaction with previous work on the inverse mirror reaction, $B^{11}(d,n)C^{12}$, yields information on the reaction mechanisms involved in these two reactions.

II. GAMMA RAYS FROM $C^{12} + p$

A. Experimental Procedure

The general experimental arrangement has been altered slightly from that used in work of a similar nature⁵ done at this laboratory. As in previous work, the Princeton synchrocyclotron beam was focused by two quadrupole lenses, brought out through a concrete and iron shielding wall, and collimated by two graphite collimators before passing through the target to the carbon-lined Faraday cup. However, the present beam tube was about twice as long as the previous one so that the target was 75 cm from the closest slit and from the Faraday cup—about twice as far as before. For this reason it was possible to shield the NaI(Tl) crystal more efficiently, giving a considerable reduction in the low-energy background. As before, the background

² W. Daehnick and R. Sherr (to be published).

³ J. K. Dickens, D. A. Haner, and C. N. Waddell, *Bull. Am. Phys. Soc.* **7**, 285 (1962).

⁴ J. S. Nodvik, C. B. Duke, and M. A. Melkanoff, *Phys. Rev.* **125**, 975 (1962).

⁵ S. G. Cohen, P. S. Fisher, and E. K. Warburton, *Phys. Rev.* **121**, 858 (1961).

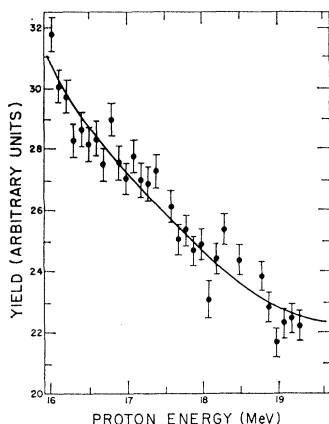


FIG. 2. The 90° yield of the 4.43-MeV gamma ray from $C^{12}+p$. Note the suppressed zero on the ordinate scale.

corresponding to about 12-MeV gamma rays and above was almost entirely due to cosmic rays.

The gamma-ray detector consisted of a 4-in. long by 5-in. diam NaI(Tl) crystal optically coupled to a Dumont 6363 photomultiplier tube. The NaI(Tl) crystal viewed the target at 90° to the beam and at distances from it of 7.5 to 23 cm. The crystal was shielded on all sides but the front by 4 in. of lead and was shielded from the collimator and Faraday cup by 8 in. of lead. The low-energy background consisted almost entirely of the 4.43-MeV gamma ray from $C^{12}(p,p')C^{12}$. With this shielding arrangement the background due to this gamma ray was reduced to less than 5% of the yield obtained from a 85-keV thick polystyrene (C_nH_n) target with 18-MeV protons. A gamma-ray spectrum taken at a proton energy of 19.8 MeV using the 85-keV thick polystyrene target is shown in Fig. 1. The 4.43- and 15.1-MeV gamma rays from $C^{12}(p,p'\gamma)C^{12}$ are indicated. In Fig. 1, the semiplateau in the pulse-height region from about channels 60 to 90 is due to pile-up. The main problem encountered in this work

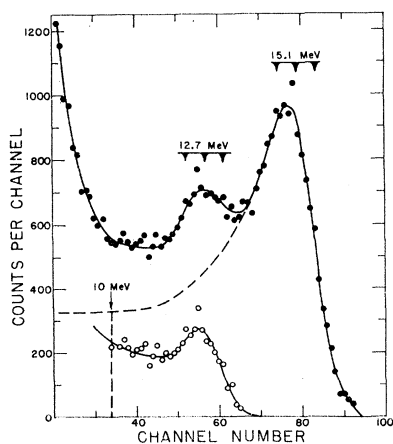


FIG. 3. Pulse-height spectrum showing the 12.7- and 15.1-MeV gamma rays from $C^{12}(p,p'\gamma)C^{12}$. The spectrum was taken at $E_p=18.8$ MeV with a 5-in. \times 4-in. NaI(Tl) crystal placed at 90° to the beam and with a bias of 6.2 MeV. The dashed line shows the assumed shape of the 15.1-MeV spectrum. The open circles are the difference between the closed circles and the dashed curve.

was reducing this pile-up which arises from the very intense 4.43-MeV gamma ray, so that the relatively weak gamma rays above 12 MeV could be studied. This was done by using low beam intensities, no more than $5 \times 10^{-4} \mu A$, and by clipping the photomultiplier output pulse to 2×10^{-7} sec and feeding the pulses into a transistorized preamplifier with a variable bias before lengthening and feeding them to the pulse-height analyzer. The cosmic-ray background, and any other background which was not prompt with respect to the beam, was reduced by gating the analyzer with a 10% time window centered about the $\sim 4\%$ duty cycle beam pulse from the synchrocyclotron. All the gamma-ray work was done using polystyrene targets which were either 500 or 85 keV thick for 18-MeV protons.

The spectral response of the 4 \times 5 in. NaI(Tl) crystal for 12- to 20-MeV gamma rays was determined from previous work,⁵⁻⁸ and from decomposing spectra like Fig. 1. For most of the spectra the yield for each gamma ray observed was determined by decomposing the

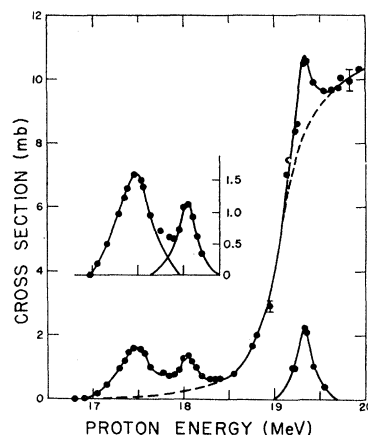


FIG. 4. The 90° differential cross section for the 15.1-MeV gamma rays from $C^{12}+p$ obtained using a 5-in. \times 4-in. NaI(Tl) crystal. The ordinate scale gives the total cross section ($\pm 20\%$), if the gamma rays have an isotropic distribution relative to the proton beam. The resonances at 17.5, 18.05, and 19.3 MeV have been emphasized by plotting the difference between the actual curve and the smoothed (dashed) curve.

spectra into individual line shapes and for each line shape summing the counts corresponding to the higher energy third of its pulse-height spectrum. The fraction of the total number of counts which was in this sum was estimated from the spectral response of the crystal. This fraction was assumed to vary linearly from 55% for 12-MeV gamma rays to 45% for 20-MeV gamma rays.

Two methods were used to obtain the absolute cross sections. First, the counting efficiency was obtained

⁵ H. W. Koch and J. M. Wickoff, National Bureau of Standards Report No. 5866 (unpublished).

⁷ R. W. Kavanagh and C. A. Barnes, Phys. Rev. **112**, 503 (1958).

⁸ E. Almquist, D. A. Bromley, A. J. Ferguson, H. E. Gove, and A. E. Litherland, Phys. Rev. **114**, 1040 (1959).

from the estimate of the fraction of gamma-ray counts summed, calculated NaI efficiencies,⁹ the weight of the target, the counting geometry, and the integrated charge. The cross-section scale obtained in this manner was estimated to have an uncertainty of 30% in addition to the uncertainties in the yield of gamma rays, the latter uncertainties being due to background subtraction and statistics. Secondly, the relative 90° yield of 15.1- and 4.43-MeV gamma rays was determined from several spectra taken between proton energies of 19.4 and 19.9 MeV such as the one shown in Fig. 1. Then the 90° differential cross section for 15.1-MeV gamma rays was determined from the known total cross section¹⁰ for the $C^{12}(p,p')C^{12}(4.43\text{-MeV level})$ reaction, an angular distribution measurement of the 4.43-MeV gamma rays at $E_p = 18.7$ MeV,¹¹ and relative 90° yields for the 4.43-MeV gamma ray for $E_p = 18.7$ –19.9 MeV. The 4.43-MeV gamma-ray yield was obtained using the experimental setup which is described

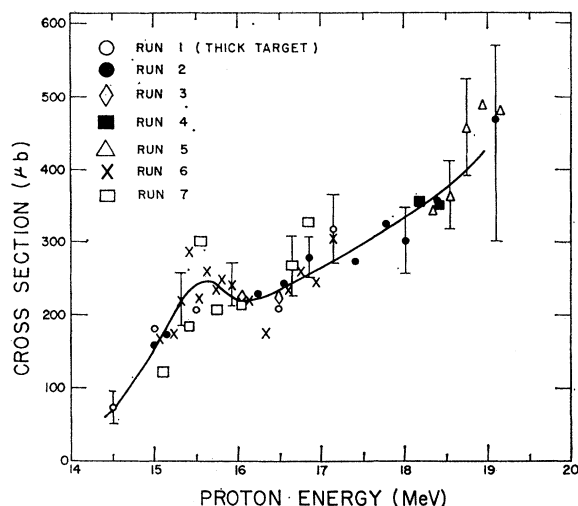


FIG. 5. The 90° differential cross section for the 12.7-MeV gamma rays from $C^{12} + p$ obtained using a 5-in. \times 4-in. NaI(Tl) crystal. The ordinate scale gives the total cross section ($\pm 20\%$), if the gamma rays have an isotropic distribution relative to the proton beam.

here and is shown for $16 < E_p \leq 19.2$ MeV in Fig. 2. The angular distribution which was measured several years ago using almost the same geometry as that used in the present work, shows a strong anisotropy with a minimum at 90° and a maximum at about 40°—an angular distribution quite similar to that obtained by the Chalk River group at $E_p = 6.9$ MeV.¹² The angular distribution indicated that the total cross section in mb is equal to (1.33 ± 0.1) times the differential cross section at 90° in $\text{mb}/4\pi$ sr at $E_p = 18.7$ MeV with the geometry used in the present work.

⁹ E. A. Wolicki, R. Jastrow, and F. Brooks, Naval Research Laboratory Report 4833, 1956 (unpublished).

¹⁰ R. W. Peelle, Phys. Rev. **105**, 1311 (1957).

¹¹ R. Sherr (private communication).

¹² H. E. Gove, A. E. Litherland, and R. Batchelor, Nuclear Phys. **26**, 480 (1961).

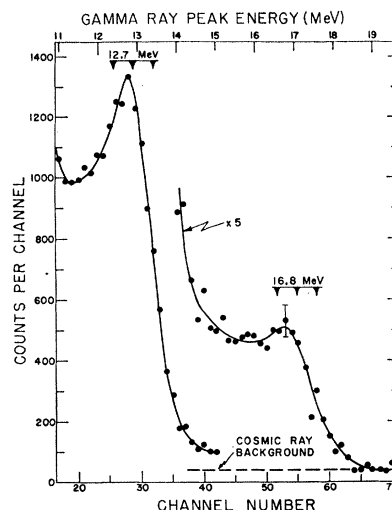


FIG. 6. Pulse-height spectrum showing the 12.7-MeV gamma rays from $C^{12}(p,p'\gamma)C^{12}$ and the gamma rays from $C^{12}(p,\gamma_0)N^{13}$ for 16.3-MeV protons incident on a 500-keV thick polystyrene target. The spectrum was taken with a 5-in. \times 4-in. NaI(Tl) crystal placed at 90° to the beam and with a bias of 8.3 MeV.

The $C^{12}(p,p')C^{12}(4.43\text{-MeV level})$ total cross sections reported by Peelle are equal within the errors of about 4% from 17.9 to 19.4 MeV, and the cross section was assumed to be constant up to a proton energy of 19.9 MeV. The 90° yield curve for the 4.43-MeV gamma ray indicated a drop in the 90° differential cross section of $(5 \pm 5)\%$ from $E_p = 18.7$ to $E_p = 19.9$ MeV.

From these data the 90° cross-section scale for the $C^{12}(p,p'\gamma)C^{12}$ reaction proceeding through the 15.1-MeV level was determined to $\pm 20\%$. This cross-section scale is 15% lower than that given by the first method which is agreement within the uncertainties of both methods. Because of its greater accuracy and reliability, the cross-section scale determined by comparison of the 4.43- and 15.1-MeV gamma-ray intensities was adopted.

B. Results

1. Excitation of the C^{12} 15.1-MeV Level

Figure 3 shows a pulse-height spectrum of gamma rays from the 85-keV polystyrene target taken with

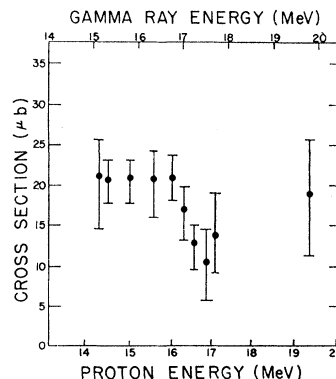


FIG. 7. The 90° differential cross section for $C^{12}(p,\gamma_0)N^{13}$ obtained using a 5-in. \times 4-in. NaI(Tl) crystal at 90° to the proton beam. The ordinate scale gives the total cross section ($\pm 20\%$), if the gamma rays have an isotropic distribution relative to the proton beam.

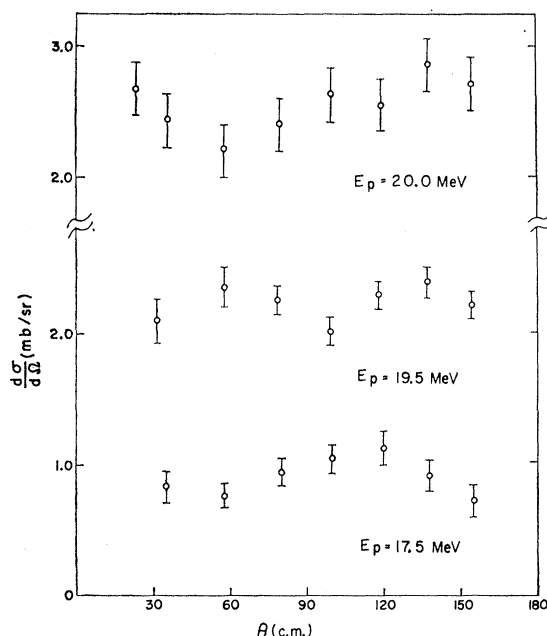


FIG. 8. $C^{12}(p,p')C^{12}$ (12.7-MeV level) angular distributions at the designated incident proton energies.

18.8-MeV protons and with a bias of 6.2 MeV. The dashed curve shows the assumed shape of the 15.1-MeV gamma-ray pulse-height spectrum. The presence of the 12.7-MeV gamma ray from the $C^{12}(p,p')C^{12}$ (12.7-MeV level) reaction is also apparent. The sum of counts determined by the assumed pulse-height spectrum to the right of the pulse height corresponding to 10 MeV were used to obtain the 90° differential cross section for the production of 15.1-MeV gamma rays. The cosmic-ray background is flat at about 8 counts per channel.

The 90° excitation curve for the 15.1-MeV gamma rays was obtained from spectra like that of Fig. 3 taken between the threshold for the reaction ($E_p = 16.35$ MeV) and 19.9 MeV. The result is shown in Fig. 4. As is clear from the representative error bars the relative cross section could be obtained quite accurately for the 15.1-MeV gamma ray because this gamma ray is quite intense relative to the background and because the background can be determined quite accurately in the energy region of interest.

The relative uncertainty of the proton energy in Fig. 4 is about 25 keV. The absolute energy scale is uncertain to 100 keV. Figure 4 is the accumulation of five separate runs. Each run was calibrated in energy relative to the others by going over the resonance seen at a proton energy of 17.5 MeV in Fig. 4.

The 15.1-MeV gamma ray was not observed for proton energies less than 16.8 MeV. An upper limit of $20 \mu\text{b}/4\pi \text{ sr}$ is set on the cross section for $16.3 < E_p < 16.8$ MeV. At 16.8 MeV the cross section was measured to be $10 \pm 5 \mu\text{b}/4\pi \text{ sr}$ and at 16.9 MeV, $20 \pm 8 \mu\text{b}/4\pi \text{ sr}$.

Three resonances are apparent in Fig. 4. To emphasize these resonances, the difference between the actual excitation curve and a smooth extrapolation of the trend of the curve is shown. These resonances are too narrow to be due to variations in the direct-interaction cross section for, in other words, the optical potential cannot vary so rapidly. Therefore, they are presumably due to compound nucleus states in N^{13} . The resonances occur at proton energies of 17.5, 18.05, and 19.3 MeV. If each resonance is due to a single compound nucleus state, then they correspond to N^{13} states at 18.1, 18.65, and 19.8 MeV. If the background represented by the dashed curve in Fig. 4 is correct, these resonances have experimental widths of 420 ± 30 , 230 ± 30 , and 250 ± 40 , respectively. The beam spread of the cyclotron is about 200 keV so that the 18.05- and 19.3-MeV resonances have total widths comparable to the beam spread. For these resonances only a limit of less than 200 keV can be given for the center-of-mass widths. For the 17.5 MeV resonance the center-of-mass width is extracted assuming the width of the 18.05-MeV resonance represents the experimental beam spread. The result is 330 ± 100 keV.

2. Excitation of the C^{12} 12.7-MeV Level

The 90° yield curve of the 12.7-MeV gamma ray was also obtained from spectra similar to that shown in Fig. 3. The uncertainty in the relative yield was considerably greater than for the 15.1-MeV gamma ray because of the presence of that gamma ray and the larger background at gamma-ray energies below 12 MeV. For many of the spectra the relative intensity of the 12.7-MeV gamma ray was obtained from the relative peak intensities of the 12.7- and 15.1-MeV gamma-ray spectra.

The 90° yield curve of the C^{12} 12.7-MeV gamma ray is shown in Fig. 5 which gives the results of seven different runs. The first run was performed with the 500-keV thick target. The 90° yield of the 12.7-MeV gamma ray shows considerably less variation with energy than the 15.1-MeV gamma-ray yield. There is a suggestion in Fig. 5 of an anomaly at a proton energy of 15.6 MeV; however, the uncertainties are too large to allow a definite conclusion to be drawn about the existence of a resonance at this proton energy. The threshold for formation of the C^{12} 12.7-MeV state by inelastic proton scattering is 13.8 MeV. The yield curve of Fig. 5 seems consistent with a threshold at this energy.

3. The $C^{12}(p,\gamma_0)N^{13}$ Reaction

The energy of the ground-state gamma rays (γ_0) following the capture of protons by C^{12} is $(1.941 + 0.924E_p)$ MeV. This is also the excitation energy of the N^{13} compound nucleus. For our maximum proton energy of 20 MeV the excitation energy in N^{13} is 20.44 MeV which is below the expected position of the photo-

nuclear giant resonance. Thus, the cross section of the $C^{12}(p,\gamma_0)N^{13}$ reaction for $14 < E_p < 20$ MeV was expected to be quite small, and this was found to be the case. The 90° yield of this reaction was investigated using the 500-keV thick polystyrene target. A spectrum obtained with 16.3-MeV protons incident on the thick target is shown in Fig. 6. At this proton energy the C^{12} 15.1-MeV level is not excited. The presence of the 12.7-MeV gamma ray and a gamma ray at about 16.8 MeV is apparent in Fig. 6. The 16.8-MeV gamma ray is ascribed to the $C^{12}(p,\gamma_0)N^{13}$ reaction. From spectra like that of Fig. 6 the 90° yield of the $C^{12}(p,\gamma_0)N^{13}$ reaction was obtained relative to either the 12.7- or 15.1-MeV gamma-ray intensities. The result is given in Fig. 7. The yield was not obtained for proton energies between about 17 and 19 MeV, because the gamma ray from this reaction was badly obscured by the much more intense 15.1-MeV gamma ray in this proton energy region. The yield curve of Fig. 7 shows little structure except for a suggestion of a minimum at a proton energy of about 17 MeV.

III. LOW-ENERGY PROTONS AND DEUTERONS FROM $C^{12} + p$

A. Experimental Procedure

Proton and dueteron angular distributions were measured in the Princeton 60-in. scattering chamber¹³ using a p - n junction detector for incident proton energies of 17.5–20 MeV. An RCA type C 20 000 Ω -cm silicon-encased junction detector was mounted on the rotating bed of the chamber. Pulses from this detector were fed into a modified Higginbotham cascade charge-sensitive preamplifier which was also mounted inside the scattering chamber. A $\frac{1}{8}$ -in. brass collimator was placed in front of the detector. Output pulses from the preamplifier were fed into a RIDL 200-channel analyzer using the incorporated A-261 amplifier.

The thickness of the active counting volume in the junction was changed by varying the applied reverse bias voltage between 10 and 130 V, excessive back current occurring above the latter voltage. An energy resolution of around 3%, full width at half-maximum, was obtained using a Po^{210} 5.30-MeV α source, greater resolution being unnecessary due to the energy spread of the cyclotron beam.

The junction bias was chosen in such a way that the desired peak in a pulse-height spectrum would not overlap other peaks and so the background under the peak could be subtracted unambiguously. Since it was not possible to stop elastically scattered protons and protons from the first excited state of C^{12} within the junction counting volume for all values of the scattering angle, it was necessary in some runs to reduce the junction bias to less than 40 V in order to display the desired peak at a higher pulse height than the peaks due to the above groups.

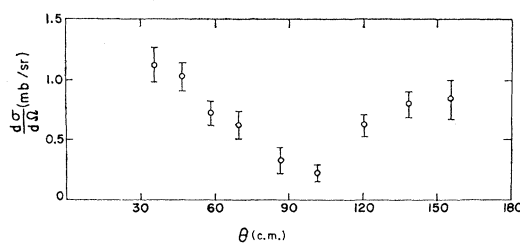


FIG. 9. The $C^{12}(p,p')C^{12}$ (15.1-MeV level) angular distribution at $E_p = 19.5$ MeV.

All runs were normalized to a given incident proton flux by measuring the collected charge. The targets were commercially available 1.2 mg/cm² and 0.7 mg/cm² polystyrene films, the latter being used exclusively for the (p,d) runs. The targets were mounted on a rotating target holder in the center of the scattering chamber.

The inelastic proton and deuteron peaks were identified within ± 150 keV of their expected energy position at all scattering angles. Energy calibration was obtained with the 5.30-MeV alpha peak from a Po^{210} source mounted inside the scattering chamber on a moveable arm. After initial warmup, the drift in the electronics was never greater than 2% between calibration runs. In addition, identification of the deuteron peak at 20-MeV proton bombarding energy was confirmed at a laboratory angle of 40° by degrading the deuteron energy with three thicknesses of aluminum, 0.35, 0.50, and 1.00 mils. The observed energies of the degraded deuterons fell within 100 keV of the predicted energies.

To evaluate the absolute cross sections in all but the 20-MeV bombarding energy runs, the net counts in a given peak were normalized to the net counts in the proton peak corresponding to the C^{12} 4.43-MeV level observed at a laboratory angle of 150° . The latter proton group was completely stopped within the sensitive counting volume of the junction at the maximum bias voltage. The values of the absolute differential cross sections for the proton group to the first excited state of C^{12} were taken from data at 17.5 MeV,² and at 19.0, 19.25, and 19.50 MeV¹⁰ incident proton energies with quoted errors of 5% and 10%, respectively. These errors are included in the values of the total absolute cross sections but not in the differential cross sections. The latter error bars indicate the standard deviations due to statistics, including background subtraction.

For data taken at $E_p = 20$ MeV, the $C^{12}(p,p')$ C^{12} (12.7-MeV level) proton group and the $C^{12}(p,d)C^{11}$ deuteron group were normalized to the elastic proton groups from carbon at laboratory angles less than 50° such that Rutherford scattering, which varies slowly with energy, would predominate. A further check on the absolute cross-section scale was made using the proton group due to elastic scattering from the hydrogen in the target at a laboratory angle of 70° ; the agree-

¹³ J. L. Yntema and M. G. White, Phys. Rev. **95**, 1226 (1954).

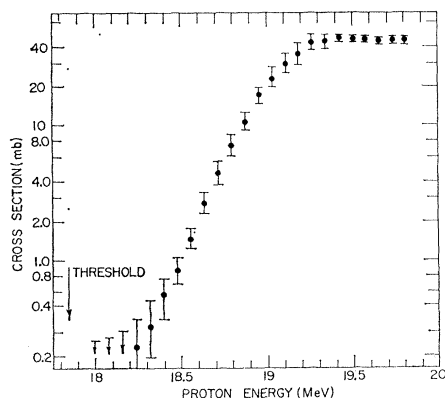


FIG. 10. Excitation curve for the $C^{12}(p,d)C^{11}$ reaction. The total cross-section scale, which is logarithmic, has an estimated uncertainty of 20%. The energy scale has an estimated uncertainty of 200 keV. The predicted threshold for the reaction is indicated.

ment with the cross-section scale obtained from the carbon group being within 15%. The absolute cross section for elastic scattering from carbon and hydrogen were obtained from data given by Peelle.¹⁰ The error in the total integrated absolute cross sections for the 20-MeV data was assigned a value of 15%, the 17.5-MeV data were assigned a value of 7% uncertainty, and the other integrated cross sections were assigned a 10% uncertainty.

The $C^{12}(p,d)C^{11}$ excitation curve was obtained using the stacked foil technique. Polystyrene foils of about 80-keV thickness for protons with energies between 18–20 MeV were accurately weighed, and a stack of 10 of these foils was bombarded for about 1 h at a given proton bombarding energy. Then the 20-min C^{11} positron activity of the foils was counted sequentially for a period of about five half-lives. The most troublesome background activity was the 10-min N^{13} activity presumably from the $C^{13}(p,n)N^{13}$ reaction. The N^{13} activity could be corrected for with negligible error except for the proton energies within 0.5 MeV of the $C^{12}(p,d)C^{11}$ threshold. Three bombardments at $E_p = 19.81$, 19.35, and 18.72 MeV covering the region between $E_p = 19.81$ and 18.0 MeV were made.

B. Results

1. $C^{12}(p,p')C^{12}$ (12.7- and 15.1-MeV Levels)

Figure 8 gives the differential cross section in the center-of-mass system for the $C^{12}(p,p')C^{12}$ (12.7-MeV level) reaction. The top, middle, and bottom curves are at proton bombarding energies of 20.0, 19.5, and 17.5 MeV, respectively. The angular distribution for the $C^{12}(p,p')C^{12}$ (15.1-MeV level) reaction at 19.5-MeV bombarding energy is given in Fig. 9. The data for these figures are listed in Tables I and II. The absolute integrated cross sections for the inelastic proton measurements are given in Table III.

TABLE I. Differential cross sections in the center-of-mass system for the $C^{12}(p,p')C^{12}$ (12.7-MeV level) at the proton bombarding energies indicated. The angles are in degrees and the differential cross sections in mb/sr.

θ	$E_p = 17.5$ MeV		$E_p = 19.5$ MeV		$E_p = 20.0$ MeV	
	$\sigma(\theta)$	$\Delta\sigma(\theta)$	$\sigma(\theta)$	$\Delta\sigma(\theta)$	$\sigma(\theta)$	$\Delta\sigma(\theta)$
23	2.68	0.20
31	2.10	0.16
35	0.84	0.10	2.43	0.21
57	0.76	0.08	2.36	0.14	2.21	0.19
79	0.95	0.09	2.27	0.10	2.40	0.20
99	1.05	0.10	2.03	0.12	2.64	0.17
118	1.13	0.12	2.31	0.10	2.56	0.16
137	0.92	0.10	2.41	0.11	2.87	0.19
153	0.74	0.10	2.33	0.10	2.72	0.20

The angular distributions given in Figs. 8 and 9 are considerably flatter than the majority of inelastic proton angular distributions obtained in the energy region of $E_p = 17$ –20 MeV.¹ This is presumably related to the high excitation energy of the levels excited. It might be possible to fit these angular distributions with the distorted wave Born approximation theory of direct interactions; however, the symmetry about 90° of the $C^{12}(p,p')C^{12}$ (15.1-MeV level) angular distributions is suggestive of the compound nucleus reaction mechanism. Results on the $C^{12}(p,p')C^{12}$ (15.1-MeV level) reaction at $E_p = 19.2$ MeV with poor counting statistics indicate that the back-angle peak in the differential cross section is considerably reduced relative to the forward-angle peak. This could be due to a contribution from the direct interaction mechanism or to the compound nucleus mechanism with interference between two or more resonances.

2. $C^{12}(p,d)C^{11}$

The excitation curve for the $C^{12}(p,d)C^{11}$ reaction which was measured by the stacked foil technique is shown in Fig. 10. The cross-section scale for this

TABLE II. Differential cross sections in the center-of-mass system for the $C^{12}(p,p')C^{12}$ (15.1-MeV level) reaction at $E_p = 19.50$ MeV. The angles are in degrees and the differential cross sections in mb/sr.

θ	$\sigma(\theta)$	$\Delta\sigma(\theta)$
36	1.12	0.15
47	1.03	0.11
58	0.73	0.10
69	0.61	0.13
86	0.33	0.11
102	0.22	0.07
120	0.63	0.09
138	0.80	0.10
155	0.85	0.16

excitation curve was obtained from the result of an integration of the $C^{12}(p,d)C^{11}$ differential cross section measured at $E_p = 20.0$ MeV. It was assumed that the cross section at 19.81 MeV, which is the highest energy

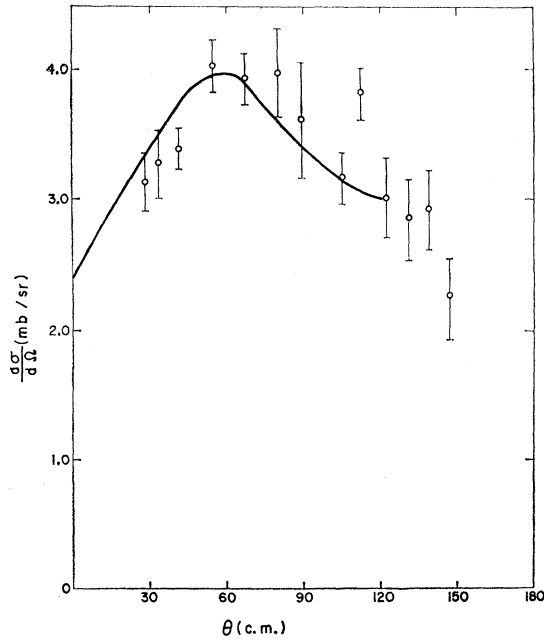


FIG. 11. The $C^{12}(p,d)C^{11}$ angular distribution at $E_p=20.0$ MeV. The solid line is the $B^{11}(d,n)C^{12}$ relative differential cross section given in reference 15 at 2.4-MeV incident deuteron energy normalized to give the best fit.

point in Fig. 10, is the same as at 20.0 MeV to within about 14%. The cross-section scale of Fig. 10 is assigned an uncertainty of 20%. The predicted threshold ($E_p=17.85$ MeV) for the reaction is indicated in Fig. 10. The cross section near threshold was too small to measure by the method used, presumably because of the effect of the Coulomb barrier on the outgoing deuterons.

The flattening out of the excitation curve between 19.3 and 19.8 MeV is in disagreement with a previous measurement¹⁴ of the $C^{12}(p,d)C^{11}$ excitation curve. The reason for this disagreement is not known.

Figures 11–13 give the results of the measurements of the absolute differential cross sections for the $C^{12}(p,d)C^{11}$ reaction in the center-of-mass system at $E_p=20.0$, 19.5, and 19.3 MeV, respectively.

TABLE III. Absolute integrated cross sections for the $C^{12}(p,p')C^{12}$ (12.7-MeV level) and $C^{12}(p,p')C^{12}$ (15.1-MeV level) reactions in the center-of-mass system.

E_p (MeV)	σ (mb)
12.7-MeV state	
17.5	11.2 ± 1.0
19.5	28.5 ± 3.0
20.0	31.0 ± 5.0
15.1-MeV state	
19.50	8.30 ± 1.0

¹⁴ W. K. H. Panofsky and R. Phillips, Phys. Rev. **74**, 1732 (1948).

TABLE IV. Differential cross section in the center-of-mass system for the $C^{12}(p,d)C^{11}$ reaction at the proton bombarding energies indicated. The angles are in degrees and the cross sections in mb/sr.

θ	$\sigma(\theta)$	$\Delta\sigma(\theta)$
$E_p=20.0$ MeV		
28	3.12	0.22
33	3.27	0.26
41	3.38	0.16
54	4.02	0.16
67	3.92	0.18
80	3.96	0.35
89	3.61	0.45
105	3.16	0.18
112	3.81	0.18
122	3.00	0.28
131	2.85	0.27
139	2.92	0.30
147	2.25	0.27
$E_p=19.5$ MeV		
28	3.61	0.25
42	3.60	0.11
55	3.17	0.06
69	2.82	0.08
81	2.80	0.11
93	2.62	0.14
106	2.23	0.18
115	1.80	0.18
$E_p=19.3$ MeV		
31	3.20	0.19
43	3.00	0.18
57	2.50	0.10
71	2.70	0.10
84	2.65	0.10
94	2.49	0.14

The data for these figures are listed in Table IV. For comparison, two relative differential cross sections of the inverse mirror reaction $B^{11}(d,n)C^{12}$ as reported by Owen and Mandansky¹⁵ are given by the solid lines

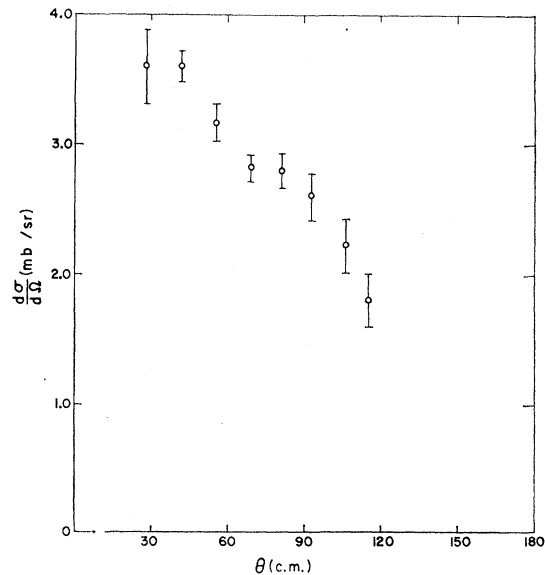


FIG. 12. The $C^{12}(p,d)C^{11}$ angular distribution at $E_p=19.5$ MeV.

¹⁵ G. E. Owen and L. Mandansky, Phys. Rev. **105**, 1766 (1957).

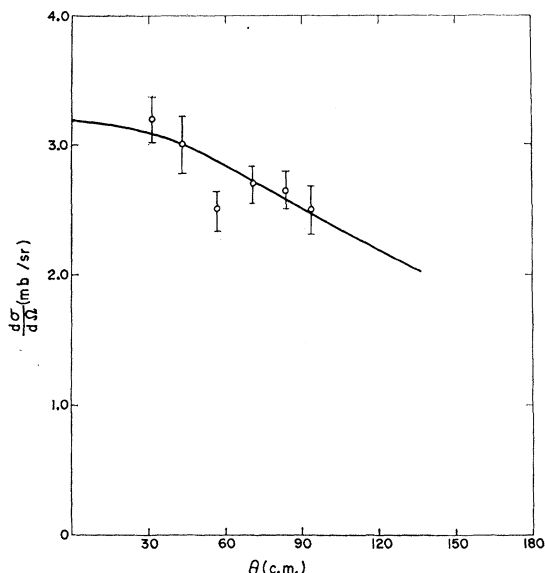


FIG. 13. The $C^{12}(p,d)C^{11}$ angular distribution at $E_p = 19.3$ MeV. The solid line is the $B^{11}(d,n)C^{12}$ relative differential cross section given in reference 15 at 1.6-MeV incident deuteron energy normalized to give best fit.

at corresponding total energies in the center-of-mass system in Figs. 11 and 13. The incident deuteron laboratory energies for the $B^{11}(d,n)C^{12}$ reaction are 2.4 and 1.6 MeV corresponding, respectively, to $E_p = 20.0$ and 19.3 MeV for the $C^{12}(p,d)C^{11}$ reaction. The $B^{11}(d,n)C^{12}$ distribution curves were arbitrarily normalized in intensity to the $C^{12}(p,d)C^{11}$ data.

Due to the comparatively high negative Q value of -16.5 MeV for the $C^{12}(p,d)C^{11}$ reaction to the ground state of C^{11} , measurements could not be obtained at backward angles for the runs at $E_p = 19.5$ or 19.3 MeV, the outgoing deuterons having energies of less than 1 MeV for these angles. Hence, the absolute integrated cross section could only be taken from the 20.0-MeV data. It is 42 ± 6 mb for $E_p = 20.0$ MeV.

The rather good agreement of the angular distributions for the $C^{12}(p,d)C^{11}$ and $B^{11}(d,n)C^{12}$ angular distributions suggests that the compound nucleus reaction mechanism is of minor importance in these reactions for the following reason: The compound nuclei involved in these two reactions are N^{13} and C^{13} , respectively. The excitation energy of C^{13} involved in the $B^{11}(d,n)C^{12}$ reaction is $(18.68 + 0.846 E_d)$ MeV and for the $C^{12}(p,d)C^{11}$ reaction the excitation energy of N^{13} involved is $(1.941 + 0.924 E_p)$ MeV. It would be quite coincidental if the energy levels of these mirror nuclei at about 20-MeV excitation were shifted relative to each other so that the same compound nucleus resonances were involved in the two reactions. In addition, the excitation curve for the $C^{12}(p,d)C^{11}$ reaction (Fig. 10) does not show any evidence for compound nucleus resonances. Thus we conclude that the reaction me-

chanism involved is predominantly the stripping reaction.

An attempt to fit the $C^{12}(p,d)C^{11}$ angular distributions of Figs. 11–13 with the plane-wave Butler stripping theory was unsuccessful. Owens and Mandansky¹⁵ fitted the $B^{11}(d,n)C^{12}$ angular distributions with a mixture of a plane-wave direct (Butler) term and a plane-wave exchange (heavy-particle) stripping term. The fits for $E_d = 1.6$ and 2.4 MeV were moderately successful; however, recent work on the $B^{11}(d,n\gamma)C^{12}$ reaction¹⁶ proceeding through the C^{14} 4.43-MeV level show that, for this reaction at least, the plane-wave stripping theory is not adequate to explain the reaction, even if the exchange term is included. In contrast, the results seem to be consistent with the distorted-wave Born approximation stripping theory and it does not seem likely that inclusion of an exchange term is demanded. Assuming the distorted-wave Born approximation formalism, the agreement of the $C^{12}(p,d)C^{11}$ and $B^{11}(d,n)C^{12}$ angular distributions indicates that the distortion effects are the same in the two reactions. This does not seem surprising since the proton energy is high enough so that Coulomb effects should be small in the proton channel. In addition the deuteron channel in the two reactions involves deuterons at the same energy (center-of-mass system) incident on mirror nuclei.

IV. CONCLUSIONS

The results for the $C^{12}(p,p')C^{12}$ (15.1-MeV level) reaction show a considerable contribution from the compound nucleus mechanism for the first four MeV above the threshold for the reaction. The excitation function shows three fairly sharp compound nucleus resonances while the $C^{12}(p,p')C^{12}$ angular distribution (Fig. 9) at $E_p = 19.5$ MeV is consistent with a compound nucleus reaction mechanism (although it does not demand it) and is considerably flatter than the majority of angular distributions for low-lying levels of light nuclei.

In contrast the results for the 12.7-MeV level do not show any conclusive evidence for the compound nucleus reaction mechanism. The angular distributions measured for the $C^{12}(p,p')C^{12}$ (12.7-MeV level) reaction are relatively flat as expected, but the excitation curve shows less structure than that for the $C^{12}(p,p')C^{12}$ (15.1-MeV level) reaction for the first four MeV above their respective thresholds. Thus, we can say that both reactions have relatively low cross sections which are rising with increasing proton energy and the flat angular distributions which are expected near threshold, but only the 15.1-MeV level data give clear-cut evidence for a large contribution from the compound nucleus reaction mechanism.

The resonances seen in the $C^{12}(p,p')C^{12}$ (15.1-MeV level) reaction were not seen in the other three reactions studied. Thus, there is no evidence for the par-

¹⁶ J. B. Garg, N. H. Gale, and J. M. Calvert, Nuclear Phys. 23, 630 (1961).

ticipation of the same resonances in two or more reactions. In fact, the $C^{12}(p, \gamma_0)N^{13}$ and $C^{12}(p, d)C^{11}$ reactions, like the $C^{12}(p, p')C^{12}$ (12.7-MeV level) reaction, show no conclusive evidence for the compound nucleus reaction mechanism.

Work has been done at Oxford¹⁷ on the excitation functions for the gamma rays from the $C^{12} + p$ for a wider range of incident proton energies but with poorer resolution than the present work. In the region of overlap the Oxford data and the data presented here are in good agreement. The Oxford data for the yield of the C^{12} 15.1-MeV gamma ray show that the cross section for the $C^{12}(p, p')C^{12}$ (15.1-MeV level) reaction has a maximum at $E_p \simeq 20.5$ MeV and drops to a value of about 1/3 to 1/4 its maximum value for $E_p \simeq 24$ –30 MeV. Thus, there appears to be a broad (~ 3 MeV wide) resonance at a proton energy of ~ 20.5 MeV in the $C^{12}(p, p')C^{12}$ (15.1-MeV level) reaction. At a proton energy of 19.5 MeV the yield of the 15.1-MeV gamma ray is close to its maximum value and so the symmetry about 90° of the angular distribution (Fig. 9) of the $C^{12}(p, p')C^{12}$ (15.1-MeV level) reaction may reflect the dominance of the $E_p \simeq 20.5$ -MeV resonance.

The work on the $C^{12}(p, p)C^{12}$ and $C^{12}(p, p')C^{12}$ (4.43-MeV level) reactions²⁻⁴ indicates anomalous behavior at $E_p \simeq 15$, 17–18, and 20–21 MeV. It may be that the resonances seen in the present work at $E_p = 15.6(?)$, 17.5, 18.05, and 19.3 MeV and the broad resonance seen by the Oxford group at ~ 20.5 MeV are responsible, at least, in part, for these anomalies.

The present experiments give some information concerning the properties of the C^{12} 12.7- and 15.1-MeV levels. A gamma ray corresponding to the C^{12} 15.1 \rightarrow 4.43 cascade was not observed. Assuming an isotropic distribution of the 15.1 \rightarrow 0 (γ_0) and 15.1 \rightarrow 4.43 (γ_1) cascades, a limit $\Gamma_{\gamma_1}/\Gamma_{\gamma_0} < 0.05$ can be set from the

spectra taken in the present work. This limit is consistent with previous measurements for this ratio of 0.031 ± 0.006^8 and 0.04 ± 0.01^{18} .

Values for Γ_{γ_0}/Γ for the C^{12} 12.7- and 15.1-MeV levels can be obtained from a comparison of the $C^{12}(p, p'\gamma)C^{12}$ and $C^{12}(p, p')C^{12}$ cross sections. The C^{12} 15.1-MeV level has $J^\pi = 1^+$ while the C^{12} 12.7-MeV level is most probably¹⁹ $J^\pi = 1^+$ and this assignment we shall assume. Thus, the ground-state transitions from these levels are pure dipole with angular distributions of the form $1 + A \cos^2\theta$ with $-1 \leq A \leq 1$. We assume isotropic distributions for both gamma rays but add an uncertainty of 10% to the $C^{12}(p, p'\gamma)C^{12}$ cross sections to take account of the possible effects of gamma-ray anisotropy. With our geometry a 10% effect in the total cross section would be caused by $|A| \approx 0.4$. Combining the $C^{12}(p, p'\gamma)C^{12}$ cross-section data of Figs. 4 and 5 with the $C^{12}(p, p')C^{12}$ cross-section data of Table III, we get $\Gamma_{\gamma_0}/\Gamma = 1.15 \pm 0.3$ and 0.027 ± 0.007 for the C^{12} 15.1- and 12.7-MeV levels, respectively. These partial widths are in agreement with previous work. The best value for the C^{12} 15.1-MeV level is²⁰ $\Gamma_{\gamma_0}/\Gamma = 0.87 \pm 0.10$ while previous estimates for the C^{12} 12.7-MeV level are $\Gamma_{\gamma_0}/\Gamma = 0.02 \pm 0.01$ and $0.03 \pm 0.01^{8,19}$.

ACKNOWLEDGMENTS

We would like to thank H. L. Berk, for his assistance in taking and analyzing the gamma-ray data; D. S. Beall, who measured the $C^{12}(p, d)C^{11}$ excitation function; and P. S. Fisher, for communications concerning the Oxford data on the gamma rays from $C^{12} + p$.

¹⁸ D. E. Alburger and R. E. Pixley, Phys. Rev. **119**, 1970 (1960).

¹⁹ F. Ajzenberg-Selove and T. Lauritsen, Nuclear Phys. **11**, 1 (1959).

²⁰ S. S. Hanna and R. E. Segel, Proc. Roy. Soc. (London) **A259**, 267 (1960).

¹⁷ Private communication from P. S. Fisher.